Available online at www.sciencedirect.com
SCIENCE DIRECT
Polymer 46 (2005) 1235–1244
polymer
www.elsevier.com/locate/polymer

Rheological behaviour of polystyrene latex near the maximum packing fraction of particles

M. Pishvaei[a,b], C. Graillat[a], T.F. McKenna[a], P. Cassagnau[b,*]

[a]CNRS-LCPP/ESCPE-LYON, 43, Blvd du 11 Novembre, BP 2077,69616 Villeurbanne cedex, France
[b]Laboratoire des Matériaux Polymères et Biomatériaux - ISTIL, UMR 5627, Université Claude Bernard Lyon I, 43 boulevard du 11 novembre 1918, 69622 Villeurbanne cedex, France

Accepted 30 September 2004
Available online 8 December 2004

Abstract

Additional developments in the comprehension of the rheological behaviour of polymer latices, especially near the high critical concentration ϕ_c, are presented for two polystyrene latices of average particle diameters close to 200 nm with different electrostatic properties. Not surprisingly, there is a rapid transition in the rheological characteristics over a narrow range of polymer volume fractions as the concentration of the disperse phase increases. By examining twelve different polymer volume fractions a unique value of the critical volume concentration, ϕ_c, was found for each latex. At this point, the steady shear viscosity, dynamic modulus, and dynamic shear viscosity change dramatically. Furthermore, these critical concentrations are well confirmed by the percolation theory for the dynamic zero shear viscosity as a function of volume fraction. The Cox–Merz rule is not obeyed by these dispersions at the concentrations greater than ϕ_c. By using a controlled strain Couette rheometer with a gap of 1.2 mm, shear thickening limits were also observed for both latices. The concentration dependence of the onset shear rate for shear thickening changes near ϕ_c for each of the two latices.

Keywords: Latex; Viscoelasticity; Cox–Merz rule

1. Introduction

The rheological properties of suspensions of non-deformable particles with relatively narrow distribution have been described in the recent literature by many researchers. The volume fraction dependence viscosity of a wide variety of these dispersions is well described by the Krieger–Dougherty [1] equation, originally introduced to describe hard sphere suspensions. More recently, the rheological properties of aqueous polyurethane dispersions were reported by Flickinger et al. [2,3], who observed the development of an apparent yield stress at the highest concentrations considered (~44 vol%). It has also been shown that the rheological character of a dispersion changes from a primarily viscous response at low particle concentrations, to an elastic response at high particle concentrations. This was demonstrated by measuring the viscoelastic properties of many polymeric latices [4–9].

As the effective volume of the particle becomes more deformable, e.g. when there is a thick layer of stabilizer surrounding a hard particle, Mewis et al. [10] showed that the Krieger–Dougherty equation becomes less effective in describing the variation of the zero shear viscosity data as a function of particle concentration. For hard particles, this expression also underestimates the low shear rate relative viscosity (η_{0r}) as the maximum packing volume fraction (ϕ_m) is approached [11,12]. Under these conditions, the dispersions approach a glass transition and the Doolittle [13] equation often captures the volume fraction dependencies of η_{0r} better than that of Krieger and Dougherty equation.

Horn et al. [14] prepared dispersions of concentrated charge-stabilized polystyrene using the potassium salt of styrene-sulfonate as co-monomer. They investigated the shear rheology of this latex and demonstrated that both high frequency and high shear viscosity were dominated by hydrodynamic interactions, and were independent of the

* Corresponding author. Tel.: +33 4 72 44 62 08; fax +33 4 72 43 12 49.
E-mail address: philippe.cassagnau@univ-lyon1.fr (P. Cassagnau).

0032-3861/$ - see front matter © 2004 Elsevier Ltd. All rights reserved.
doi:10.1016/j.polymer.2004.11.047

ionic strength. They also showed that these two quantities were not identical due to the micro-structural distortion resulting from high shear.

On the other hand, the zero-shear viscosity (η_0) tends to infinity at volume fractions denoted as ϕ_m, which are well below values of 0.58–0.63 (upper limit for the volume fraction of randomly packed spheres). This range is typical for mono-dispersed dispersions of hard spheres. Furthermore at low shear, ϕ_m strongly depends on the ionic strength, which determines the range of electrostatic interactions. Rescaling the volume fraction by ϕ/ϕ_m allows one to obtain a master curve (i.e. independent of size of particles and salt concentrations) for zero-shear viscosity versus volume fraction. The same dispersions of charged stabilized polystyrene have been used for preparation of bimodal dispersion by Horn and Richtering [15]. In addition, the Cox–Merz rule, i.e. the correlation between the dynamic shear viscosity $|\eta^*(\omega)|$ and the steady shear viscosity $\eta(\dot{\gamma})$ with $\omega \equiv \dot{\gamma}$, is obeyed by solid dispersions only at strains in the linear viscoelastic region and at concentrations below the gel point where the system can obtain a Newtonian shear plateau or the onset of an apparent yield point for the system [2,3,16]. In the regions of shear thinning, the dynamic viscosity is always greater than the shear viscosity.

Another important phenomenon in highly concentrated latices is shear thickening behaviour. For example, Laun et al. [17] investigated shear thickening in non-aqueous dispersions using various types of rheometers, and concluded that the apparent critical shear rate for the onset of shear thickening depended on the rheometer geometry, but also that the viscosity change of this phenomena can be traced continuously by using a stress-controlled rheometer. Viscosities of concentrated shear thickening dispersions were measured as a function of shear rate, Couette cylinder size, and time by Boersma et al. [18,19]. At shear rates above the onset of shear thickening for $\phi > 0.57$, strong viscosity instabilities were detected, together with a dependence on cylinder size. The instabilities are attributed to reversible order–disorder transitions, e.g., from strings to clusters. This dependence on cylinder size is due to wall slip, slipping planes in this dispersion, and even plug flow in the gap. With less concentrated, or polydisperse dispersions the effects are much less severe, but thixotropic behaviour was observed nevertheless, probably due to a reordering of the dispersion. Laun [20] also measured the first and second normal stress differences for a strongly shear thickening nonaqueous polymer dispersion of 58.7 vol% of styrene and acrylate copolymer.

The rheological and microstructural properties of dense suspensions of uniform, charge-stabilized colloidal spheres were investigated by Chow and Zukoski [21,22]. Thickening was only observed above a volume fraction of 0.4–0.5, depending on particle size and the shear rates. Xu et al. [23] observed a time-dependent shear thickening phenomenon in a commercial aqueous poly(acrylic ester) dispersion. The critical shear rate for the shear thickening transition varied as a function of the volume fraction, temperature, pH, and particle size distribution, in a manner which indicates that the phenomenon is associated with a reversible shear-induced colloidal order–disorder transition. It is possible that the time-dependence is caused by the temporary formation of particle clusters at high shear rates. The authors measured the critical shear rate at which shear thickening begins for four concentrations above 57%. It has been shown that this shear rate is a strongly decreasing function of solid concentration.

Melrose et al. [24] and Catherall [25] studied the shear thickening of systems stabilized by charges and/or polymer layers using Stokesian dynamics at core volume fractions $>40\%$ (the core volume fraction refers to the fraction occupied by the particle alone, and does not include the volume of the stabilisation layer). Strong thickening behaviour was only observed in the case where a polymeric stabilizer was used. However, there remains a lack of studies on the non-Newtonian phenomena common to almost all of dense suspensions as shear thickening.

The objective of the present work is to investigate the rheological properties of concentrated polystyrene latices with different electrostatic properties around the high critical concentration. Linear viscoelasticity experiments were used to study the transition from viscous to elastic flow, and the variation of the dynamic zero shear viscosity at the gel point is discussed in terms of the percolation theory. Additionally, the critical exponent on the dynamic zero shear viscosity at the percolation threshold will be correlated with the Krieger–Dougherty equation. Furthermore, the zero shear viscosity of PS latices is discussed in terms of effective volume fraction, and the applicability of the Cox–Merz rule is examined. Finally, the shear-thickening behaviour of the two different latices is studied in terms of the critical shear rate in order to identify the shear thickening transition as a function of the volume fraction.

2. Experimental

2.1. Material preparation

The two latices were made by emulsion polymerisation using ammonium persulphate (APS) as the free radical initiator. The first latex of polystyrene homopolymer (PS) was produced in a semibatch reaction that lasted for 12 h, using Disponil® 3065 (mixture of linear ethoxylated fatty acids) as the non-ionic surfactant. The second latex (PSS) is a copolymer of styrene plus 13% by weight (with respect to total polymer) of the potassium salt of styrene sulphonate. PSS was produced directly in a batch reaction using Triton 405X as the non-ionic surfactant. The major different between the two latices is the presence of strong acid groups on the surface of PSS with a dissociation constant similar to that of the initiator. These acid groups will change the degree of the hydrophilicity of the particle surface.

Table 1
Synthesis and properties of polystyrene latex

Sample	Size (nm)	PDI	Solid (%)	Styrene (g)	H_2O (g)	No ionic surfactant (g)	$(NH_4)_2SO_4$ (g)	Styrene sulfonate (g)	pH
PS	194	0.07	46.7	500	500	34 (65%) (Disponil)	0.7	0	2.18
PSS	211	0.07	54.07	511	400	6.6 (70%) (Triton)	0.7	6.6	2.56

Samples with different polymer concentrations were prepared either by diluting the original latex with different amounts of deionised water, or by concentrating it by vacuum distillation. Weight fractions were converted to volume fractions using a density of 1.045 (g/cm^3). No salt was added for the preparation of this series. The different parameters for the latex synthesis are reported in Table 1.

The average particle size was determined by quasi-elastic light scattering (QELS) on a Lo-C from Malvern Instrument Corporation (Villeurbanne, France). A polydispersity index (PDI) is provided by the software, which, according to the manufacturers, indicates that the latices can be considered to be relatively monodisperse and that the value of size is valid if the PDI <0.1. In Table 1, both of the latices can be considered to be monodisperse, and have similar average diameters. Thus any differences between the measured rheological parameters of these products can be attributed to interactions between the particles, and not to the influence of the particle size distribution (PSD).

Conductimetric titration of the acid groups on the particle surface was done using an automatic titration instrument controlled by a CDM 83 conductivity meter, and using a NaOH solution (0.01 N) as the titrant. To do this measurement, the dispersions were first treated 4–5 times with an ion exchange resin (Dowex MR-3) for 1–2 days. The diluted dispersions were purged thoroughly with nitrogen to prevent absorption of carbon dioxide from the air before and during titration.

Electrophoretic mobility was determined using a Malvern instrument ZetaSizer 3 for the two latices diluted with KCl (10^{-3} M) at neutral pH since Horn et al. [14] noted for this system of polystyrene latices that the variation of the pH between 4 and 9 did not lead to any significant changes in the electrophoretic mobility. The results from the comparative characterization are summarized in Table 2.

2.2. Rheological measurements

Steady shear viscosity, dynamic deformation sweep and frequency sweep curves were obtained using a controlled strain Couette rheometer with an inner diameter of 32 mm, an outer diameter of 34 mm, and a cylinder length of 34 mm. All measurements were conducted at ambient temperature (23–25 °C), and the samples were covered with a thin layer of an organic oil to prevent evaporation of water.

In oscillatory measurements, one initially fixes the frequency at 6 rad/s and measures the rheological parameters as a function of strain amplitude. This enables one to reach the linear viscoelastic region where the complex shear modulus $\{G^*(\omega)=G'(\omega)+jG''(\omega), j^2=-1\}$ is independent of the amplitude of the applied strain at any given frequency. Once the linear region is established, measurements are then made as a function of frequency at certain amplitudes. Flickinger et al. [2] mentioned that in their latex system, deviation from linear viscoelasticity occurs at strains less than 0.05% for moderately concentrated dispersions of polyurethane. We observed such sensitivity with respect to linearity for the PSS latex (as we will see below, this system is very shear sensitive). For highly concentrated PS latex samples, the linear region is observed for deformations lower than 10%, whereas the linear region for PSS at medium concentrations ($\phi \geq \phi_c$) is only observed for deformation lower than 1%.

3. Linear viscoelastic behaviour

3.1. Complex shear dynamic modulus G*(ω)

The variation of the complex shear modulus versus frequency for PS latices is shown in Fig. 1(a)–(c). At concentrations lower than 55.3%, in the terminal zone of frequency or time, G' and G'' are proportional to ω^2 and ω^1 respectively. As the particle concentration is increased beyond this point, the frequency (see Fig. 1(c)) where G' crosses G'' decreases rapidly. The shift towards lower frequencies results from the increase in the relaxation time with increasing volume fraction (see Table 3). The crossover frequency ω_c where $G'=G''$ is representative of

Table 2
Physical properties of polystyrene latex

	Conductivity (μCm)	Charge per surface from titration (μC(cm^2)	Zeta potential (mV) In KCl (10^{-3})	Size (nm) In KCl (10^{-3})	Size (nm) In KCl (10^{-1})
PS	1.6	0.88	−30.4	193	Coagulation
PSS	1.9	14.59	−44.7	211	200

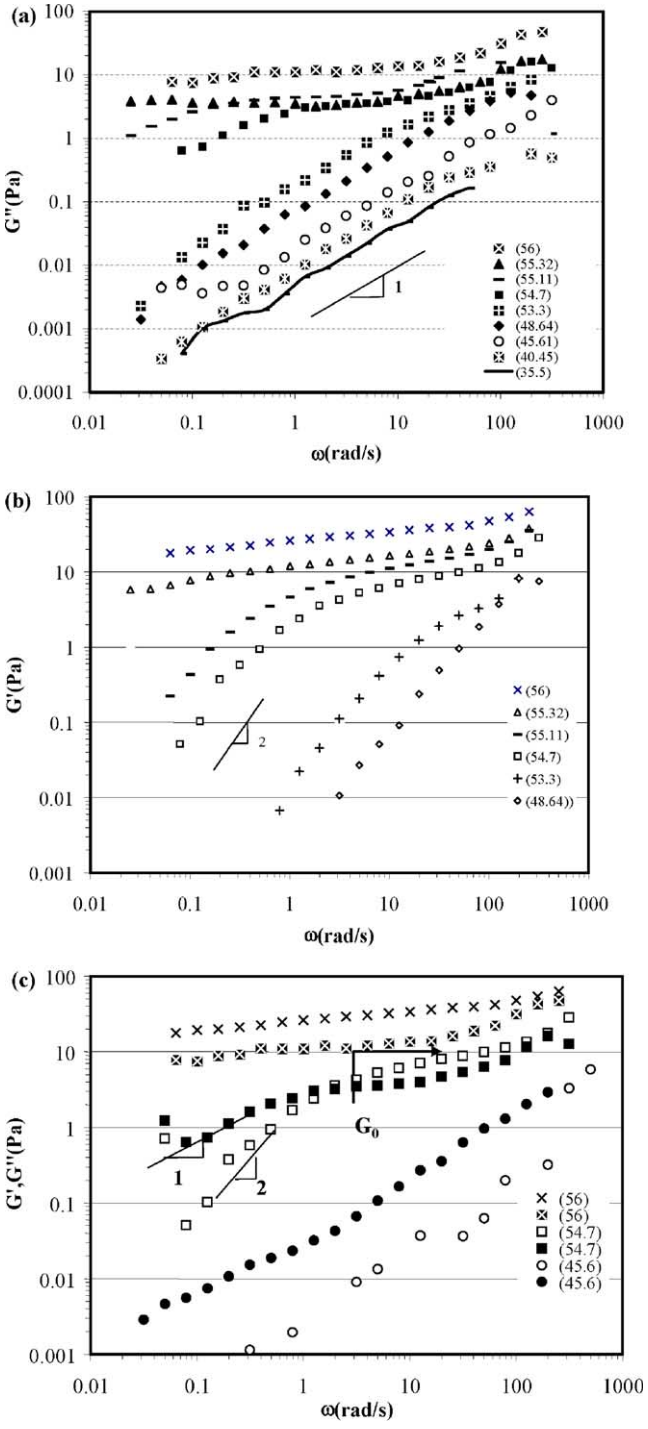

Fig. 1. Viscoelastic behaviour of latex for different PS volume fraction (%): (a) Loss modulus: $G''(\omega)$ (b) Storage modulus: $G'(\omega)$ (c) Complex shear modulus: $G^*(\omega)$ for three particular concentrations, G'' solid points and G' open points.

a characteristic relaxation time, $\tau_c = 1/\omega_c$, which corresponds to the time for a particle to diffuse a distance equal to its radius. This mean relaxation time is thus generally observed to be inversely proportional to the particle diffusivity $D_s(\phi)$.

From the terminal relaxation zone of suspensions at intermediate concentrations, we can also measure the steady state-compliance J_e^0:

$$J_e^0 = \frac{1}{\eta_0^2} \lim_{\omega \to 0} \frac{G'(\omega)}{\omega^2} \tag{1}$$

This important value is a measure of stored energy or residual strains, and is called the equilibrium recoverable compliance.

Table 3 shows that J_e^0 decreases slightly as the volume fraction of the suspension increases. The critical concentration was defined as the solid content at which the system begins to behave like an elastic solid, i.e. with $G' > G''$ over the entire experimentally accessible frequency range, and where both of modulus are nearly constant (i.e. independent of frequency). At this particular concentration, one can say that the relaxation time tends to infinity (at least in the experimentally accessible frequency domain). ϕ_c must therefore be near 55.3%, since, as discussed in the following section, the dynamic zero shear viscosity (η_0^*) is not attainable for this concentration (see Table 3) because this sample shows an apparent yield stress.

Furthermore, it can be seen from Fig. 1(c) that at a volume concentration of 54.7%, the elastic modulus exhibits a plateau at the highest frequencies. Physically, this plateau of the modulus means that all the PS particles participate in a physical network, giving a rubber-like response in that scale of frequencies. The following power law is observed for the present PS samples:

$$G_0 \propto \phi^{33} \tag{2}$$

Actually, most of the work found in the literature shows that the storage modulus approaches a constant G'_∞ at high frequencies. Furthermore, it is helpful to extract this high frequency elastic modulus from the frequency sweep in order to make a comparison between the mechanisms of glassy systems and to develop theories for the high frequency modulus of the suspension. However, we cannot define such high frequency behaviour from our work, which means that the usual theories only based on the interaction potential between particles in close contact cannot really capture the complete physics in these suspensions. In order to improve these theories, Flickinger and Zukoski [3] proved that combining the electrostatic and short range interactions provides a better description of the fraction dependence of G'_∞.

Eventually, assuming $G_0 \equiv G'_\infty$, our power law (Eq. (2)) is consistent with data reported in the literature [3,27,28].

Furthermore, the product $G_0 J_e^0$, which is a measure of the breadth of the relaxation spectrum, has practically the same value $G_0 J_e^0 \approx 2$. This means that the relaxation time distribution is rather narrow. This value is very close to those obtained for the linear polymers ($2.5 < G_0 J_e^0 < 3$) with very narrow distribution [26]. Recall that $G_0 J_e^0 = 1$ for the Maxwell model which takes into consideration only one unique relaxation time. To the best of our knowledge no

Table 3
Rheological properties of polystyrene latex

ϕ(PS) (%vol)	35.5	40.45	45.61	46.79	48.64	52.08	54.71	55.11	55.32	56
η_0^* (Pa.s)	0.005	0.009	0.023	0.03	0.056	0.2	6	30	–	–
G^0 (Pa)	–	–	–	–	–	4	7	12	15	30
J_e^0 (Pa^{-1})	–	–	–	–	1	0.5	0.25	0.2	–	–
$\tau_c = 1/\omega_c$ (s)	–	–	–	–	0.005	0.017	0.5	1	–	–
ϕ(PSS) (vol%)	38.77	39.96	43.8	45.6	46.88	47.89	48.69	49.94	51.17	52.08	52.97	54.22
η_0^* (Pa.s)	0.008	0.01	0.028	0.09	0.25	12	–	–	–	–	–	–
G_e (Pa)	–	–	–	–	–	–	–	–	3	3	5	8

such data has been reported in the literature for the relaxation spectrum of concentrated latices.

A quite different trend can be observed for the PSS latex in Fig. 2(a)–(c) and these results contrast with ones reported above for PS samples. In order to clarify these Figures, three complex shear moduli (G' and G'') curves are plotted in Fig. 2(c). This figure describes the rheological behaviour of the latex far below the critical point, around this critical point, where the viscoelastic behaviour changes, and far beyond the critical point. This critical point can be correlated to the concept of percolation threshold or sol–gel phase transition in crosslinked polymer system. Below the gel point, one observes the classical liquid behaviour ($G''\alpha\omega^1$ and $G'\alpha\omega^2$) at low frequencies. Beyond the gel point, the materials behave like viscoelastic Hookean solids at low frequencies or large scales ($G'\alpha\omega^o$; $G' = Ge = \lim_{\omega\to 0} G'(\omega)$).

The concept of percolation was extensively used for understanding the rheology of crosslinked polymer networks as for example. The transition occurs during a random aggregation process of subunits into larger and larger molecules. Scaling relations have been developed to provide the divergence of the properties at the percolation threshold [29]. On the other hand, the long-range connectivity in the emulsions may arise from physical interactions. The liquid–solid transition for suspensions in which the particles aggregate into sample-spanning complexes have the same features as for chemical gelling, namely the divergence of the longest relaxation time and power law spectrum with negative component [30].

Near the percolation threshold, the storage modulus crosses over the loss modulus, and the rheological criterion for the definition of the percolation threshold is the same power law for $G'(\omega)$ and $G''(\omega)$ [30]:

$$G'(\omega)\alpha G''(\omega)\alpha\omega^n \tag{3}$$

where n is the relaxation exponent. From this criterion, the percolation threshold can be determined for the PSS latex at the volume concentration of 47.9% with a relaxation exponent $n \approx 0.5$.

In summary, this pair of observations suggests that the presence of the electrically charged groups on the surface of PSS induce interactions between neighbouring particles. On the other hand, the PS particles behave more like rigid non-interacting spheres. A percolation threshold can be defined from a viscoelastic analysis of the complex shear modulus.

3.2. Dynamic shear viscosity (η^*)

There is another rheological parameter defined in dynamic shear tests as the dynamic shear viscosity: $\eta^*(\omega) = G^*(\omega)/j\omega$. Percolation theory has been successful in predicting the static properties of gel fragments near the gel point of crosslinked plastics [31], which will be apply for the trend of zero shear viscosity of the emulsion η_0. We used this concept of percolation (Eq. (5)) for the dynamic zero shear viscosity defined as Eq. (4):

$$\eta_0 = \lim_{\omega\to 0} \eta'(\omega) = \lim_{\omega\to 0} \frac{G''(\omega)}{\omega} \tag{4}$$

$$\eta_0 \propto (\phi_c - \phi)^{-s} \quad \text{for } (\phi < \phi_c) \tag{5}$$

According to the scaling law in Eq. (5), a plot of $\log(\eta_0)$ versus $\log(\phi_c - \phi)$ for various values of the volume fraction should allow us to confirm our experimental estimation of the critical volume fraction ϕ_c for each latex by fitting the experimental zero shear viscosity data as illustrated in Fig. 3. It is clear from Eq. (5), that both ϕ_c and s can be treated as adjustable parameters. If we plot $\log(\eta_0)$ as a function of $\log(\phi_c - \phi)$, as shown in Fig. 3, it can be seen that the best fit obtained for ϕ_c is in agreement with the values obtained from the viscoelastic tests. In addition, one can also see the sensitivity of $\log \eta_0$ to small changes in ϕ_c in this same figure.

We found the exponent's, the slope of the best-fitted straight line, can be correlated with the exponent $[\eta]\phi_m$ of the Krieger–Dougherty Eq. (6).

$$\eta_0 = \eta_s \left(1 - \frac{\phi}{\phi_m}\right)^{-[\eta]\phi_m} \tag{6}$$

It should be underlined here that ϕ_c is defined as the point where $\eta_0 \to \infty$. This is not necessarily the same thing as the maximum packing fraction, since it is possible to have higher solid concentrations than ϕ_c at infinite zero shear viscosity (see Table 3). Nevertheless, we will allow

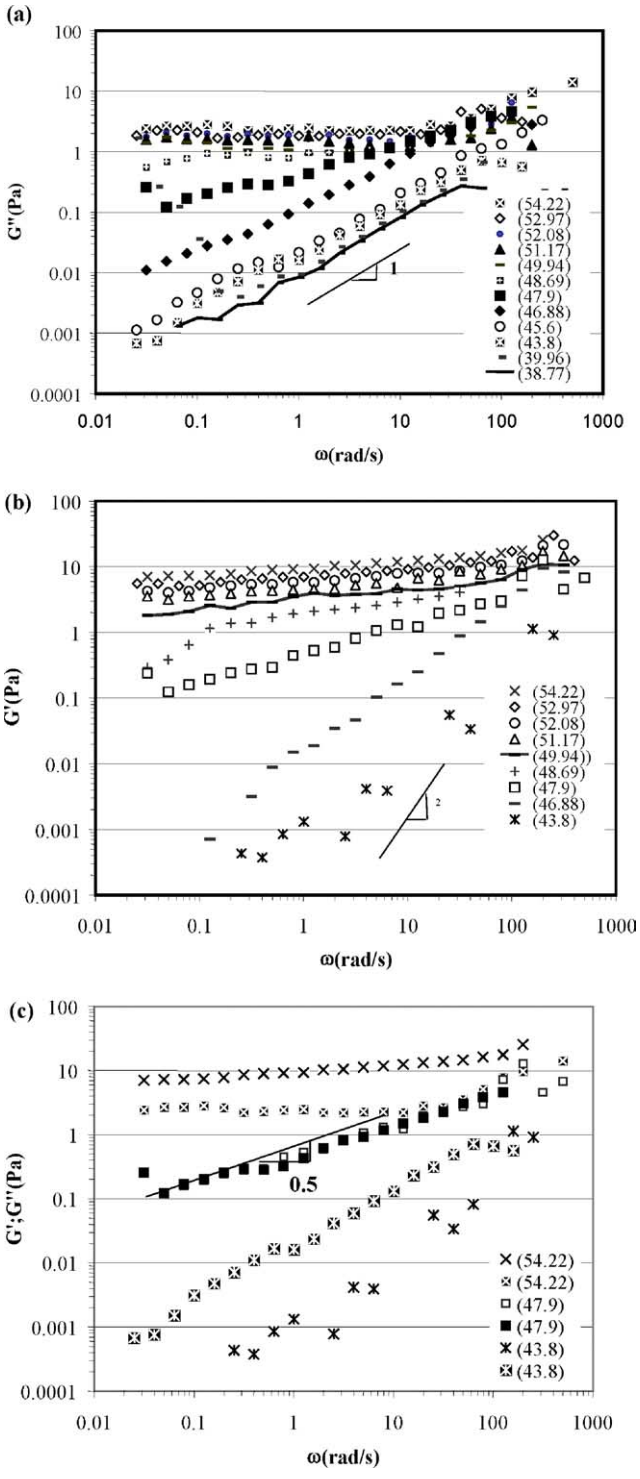

Fig. 2. Viscoelastic behaviour of latex for different PSS volume fraction (%): (a) Loss modulus: $G''(\omega)$ (b)Storage modulus: $G'(\omega)$ (c) Complex shear modulus: $G^*(\omega)$ for three particular concentrations, G'' solid points and G' open points.

ourselves to make the approximation $\phi_c \approx \phi_{m,0}$ (the packing fraction where the zero shear viscosity tends to infinite) for obvious reasons. Other packing fractions, such as the absolute maximum packing fraction, $\phi_{m,\infty}$ can be defined as the particle volume fraction where the high shear viscosity

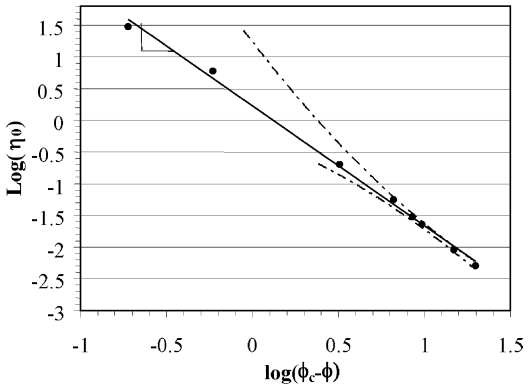

Fig. 3. Prediction of the percolation exponent s from dynamic zero shear viscosity: $\eta_0 = k(\phi_c - \phi)^{-s}$.

(high shear Newtonian plateau in the viscosity curves) tends to infinity. $\phi_{m,0,eff}$ typically lies between 52 and 57%, and $\phi_{m,\infty}$ between 60% and 63% [7].

Furthermore, $\phi_{m,0}$ strongly depends on the ionic strength which determines the range of electrostatic interactions. In contrast the high shear viscosity is essentially independent of ionic strength of latex, depending only on volume fraction [14]. Hence one tends to consider the $\phi_{m,0}$ in the viscosity–concentration models.

Let us consider Eq. (5) with $\phi_c \equiv \phi_m$ and $s \equiv [\eta]\phi_m$. Here $[\eta]$ is the intrinsic viscosity of the suspension, for rigid spheres without any electrosteric interaction $[\eta] = 2.5$. Actually the divergence of the zero shear viscosity indicates a transition from disordered fluid to an elastic solid at ϕ_c. This transition occurs as the latex concentration approaches the limit of close packing of hard spheres ϕ_m. From Fig. 3, we get $s = 1.90$ for PS, and $s = 1.65$ for PSS (see Table 4).

The value of s for PS is close to the value of 2 in the expression developed by Quemada [32]:

$$\eta_{0,r} = (1 - \phi/\phi_m)^{-2} \tag{7}$$

This is not surprising, as Eq. (7) was developed for hard, non-interacting spheres. Since the PS latex was made with non-ionic surfactant and limit electrical charges, one would expect the particles to have only minimal interactions. This is clearly not the case for PSS.

Consequently, the intrinsic viscosity of PS and PSS suspensions are $[\eta] = 3.42$ and 3.44, respectively. These values are closed to those found by Raynaud et al. [7] for emulsions of poly(butyl acrylate-styrene) with 254 nm in diameter and Zeta potential of (−37 mV) where intrinsic viscosity equal to 3.65 is clearly different from the value of 2.5 for hard spheres. This discrepancy is caused by the fact

Table 4
Experimental and theoretical critical volume fraction and intrinsic viscosity in SS and SU latex systems

Sample	ϕ_c (%)	s	$[\eta] = s/\phi_c$
PS	55.3	1.90	3.42
PSS	48	1.65	3.44

that the hydrodynamic radius of the particles is increased either by the surfactants or comonomers adsorbed on the surface or by the first electro-viscous effect due to the electrostatic charges on the surface of the particles. In addition, one cannot exclude the possibility of the presence of water-soluble molecules that will vary from recipe to recipe, and also participate in increasing the intrinsic viscosity from that of pure water.

Fig. 4 shows the variation of the relative zero shear viscosity versus volume fraction for PS and PSS. Here the solid lines represent the Krieger–Dougherty equation considering the values of percolation theory for the $[\eta]$ and ϕ_c. The relative zero-shear viscosities is defined as $\eta^*_{0,r} = \eta^*_0/\eta_s$ where η_s, is the viscosity of the continuous medium (water), and η^*_0 were determined from the dynamic shear flow curves considering the low Newtonian plateau for viscosity which are experimentally accessible so that, no extrapolations are necessary. The values of η_0 which are used for this curve are equal in both the steady and dynamic curves (η^*_0) because in our system the Cox–Merz rule is obeyed for concentration less than ϕ_c as shown later.

As previously explained, Fig. 4 shows that the zero shear viscosity diverges at a high volume fraction denoted ϕ_c, as observed by Horn et al. [14,15]. This volume fraction is below values of 0.58–0.63, typical for hard spheres. It is well known that electrostatic interactions have a large influence on the low shear viscosity, and this can explain why ϕ_c for PSS latex ($\phi_c = 47.9$) is lower than of the PS latex ($\phi_c = 55.3$). The deviation from the hard-sphere behaviour can be described in terms of an effective volume fraction. This concept of an effective volume fraction can also be used to describe the viscosity of bimodal, electrostatically stabilized latices [15].

By considering the number of surface charges determined by conductimetric titration and also the electrophoretic mobility values of the two latices considered here, it is clear that PSS has more charges on the particle surface because of its composition. Thus in Fig. 4, the different trends observed for PSS and PS can be attributed in large part to the fact that PSS has more electrically charged groups on its surface, therefore in an aqueous medium it will have more long range interactions. These will obviously have an effect on the rheology of this latex, especially for high particle concentrations.

3.3. Modelling of $\eta_0(\phi)$

In many studies the models described by Quemada, (Eq. (7)) or by Krieger and Dougherty (Eq. (6)) were used to determine ϕ_m by an extrapolation of viscosity curves [4–9,27,33,34]. In the work presented here we used the values of ϕ_c obtained from the rheological curves in percolating point of concentration, and also fitted our experiment data with Eq. (7) considering $\phi_c \equiv \phi_m$. As PSS particles act like hard particles ($T < T_g$) with thick, soft layers (of styrene sulfonate oligomers), they do not behave as predicted based on the hard sphere approximation inherent in the Quemada equation. In particular, they display a more rapid increase in η_0 as ϕ increases. The ability of Eq. (6) to describe the volume fraction dependence of η_0 also breaks down near ϕ_m where these suspensions exhibit different dynamic properties due to particle interactions [2].

In order to better compare the polystyrene and polystyrene-styrene sulfonate the concept of ϕ_{eff} described by Horn et al. [14,15] was used to include the volume of the stabilisation layer in the analysis. This effective volume fraction was determined by comparing the experimentally determined divergence of the zero shear viscosity with the hard sphere value as following formula:

$$\phi_{eff} = \phi(\phi_{max,hs}/\phi_{max,exp}) \quad (8)$$

We fitted this model by considering our finding critical volume fraction as $\phi_{max,exp}$ and taking $\phi_{max,hs}$ (maximum packing of hard sphere) equal to 0.61 as suggested in the references cited above. The points in Fig. 5 present the results for our two latices, and the solid line is the predictions of the Krieger–Dougherty model with the

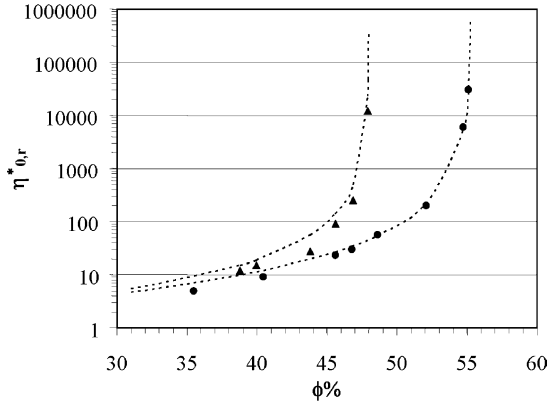

Fig. 4. Variation of the relative zero shear viscosity versus volume fraction for PS (●) and PSS (▲) latex; solid line: the curves for PS and PSS according to Krieger–Dougherty equation.

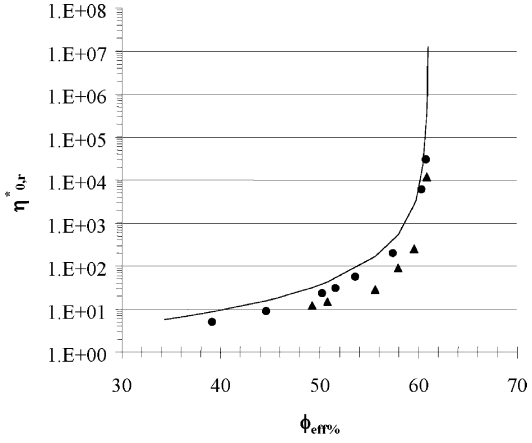

Fig. 5. Variation of the normalized zero shear viscosity versus effective volume fraction for PS (●) and PSS (▲) latex; solid line: curve for PS and PSS according to Krieger–Dougherty equation.

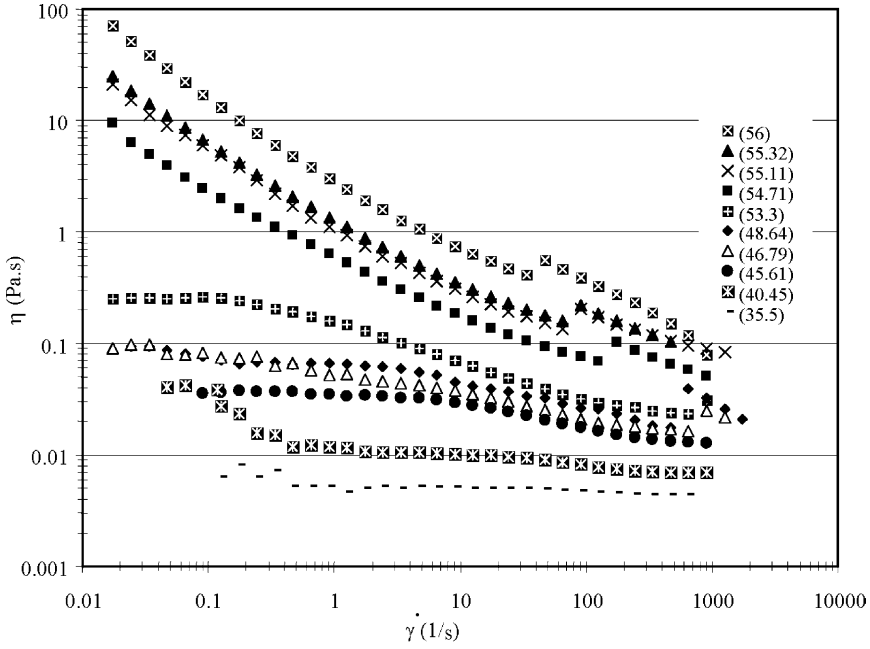

Fig. 6. Variation of the steady shear viscosity versus shear rate for PS samples at different volume fractions.

effective volume fraction and our experimental $[\eta]$ from percolation low. The slight shifting of experimental curve of PSS to the right of PS is possibly explained by the difference of about 17 nm in larger diameter of PSS. Nevertheless by considering ϕ_{eff}, we obtained a master curve for relative zero viscosity, i.e. independent of particle size and the electrostatic effect of the surface charge of the particles.

4. Non linear rheological behaviour

4.1. Steady shear viscosity

Figs. 6 and 7 show that the viscosity becomes sensitive to shear rate at low $\dot{\gamma}$ for $\phi > 44\%$. One can be seen a weak shear thinning behaviour at some concentrations below ϕ_c, while for others the plateaux of zero shear viscosity are not measurable (as expected) and a dramatic decrease in viscosity over several order of magnitudes is observed. The shear thinning behaviour occurs when the shear rate is high enough to disturb the distribution of inter-particle spacing caused by Brownian diffusion from its equilibrium level, and its onset can be connected to a dimensionless shear rate generally referred to as the Peclet number by $Pe \gg 1$.

$$Pe \equiv \tau_0 \dot{\gamma} (\phi_c - \phi)^s \tag{9}$$

In fact, Pe is a dimensionless shear rate and τ_0 is the characteristic relaxation time of a suspension in low shear rate, which is inversely proportional to the particle diffusivity [35].

Another conclusion that can be drawn from the curves of viscosity versus shear rate is that there is a critical concentration ϕ_c where the behaviour of latex changes. Below this concentration, the zero shear viscosity is well defined. At ϕ_c, the zero shear viscosity diverges and tends to infinity. Above it, the zero shear viscosity could not be measured, and the viscosity decays as $\dot{\gamma}^{-\beta}$ with $\beta \sim 1$ indicating the onset of yield stress type behaviour. Generally, the yield stress appears when the particle repulsions are strong enough to induce a regular arrangement of particles or a sort of 'macrocrystallization'. This arrangement is more probable at higher particle concentrations, and therefore stronger repulsions.

On the other hand, Fig. 8 shows that the Cox–Merz rule, where $|\eta * (\omega)| = \eta(\dot{\gamma})$, with $\omega = \dot{\gamma}$ can be verified for both latices, only when the volume fraction is lower than ϕ_c. At high concentrations ($\phi > \phi_c$) the Cox–Merz rule is not

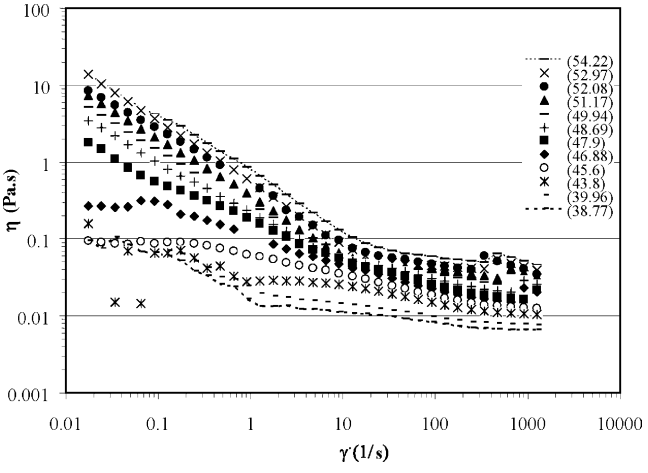

Fig. 7. Variation of the steady shear viscosity versus shear rate for PSS samples at different volume fractions.

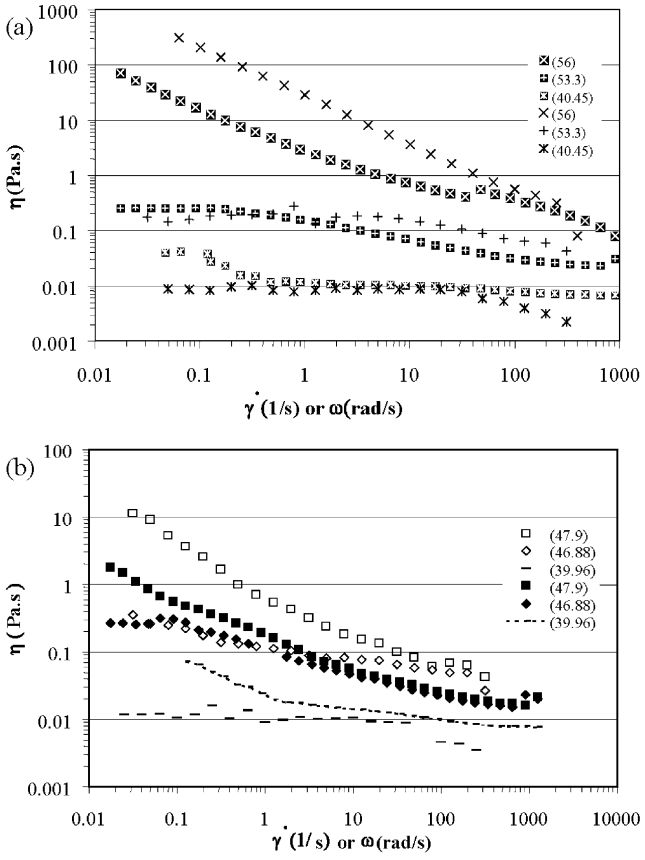

Fig. 8. Coz–Merz rule. Comparison between dynamic shear viscosity $|\eta^*(\omega)|$ and steady shear viscosity $\eta(\dot{\gamma})$ for different volume fraction. PS sample PSS sample.

obeyed. The values of the dynamic viscosity $|\eta^*|$ are always greater than the steady shear viscosity at $\omega = \dot{\gamma}$. Similar observations have been made in several structured systems [16].

However, the failure of the Cox–Merz rule can be corrected using a constant shift factor of 25, which results in excellent agreement between the shear viscosity and complex viscosity data in the system studied by Flickinger et al. [3], and also for our experimental results for $\phi > \phi_c$. This deviation from Cox–Merz rule can be explained by the fact that in steady shear flow, as opposed to dynamic shear flow, the shear distortion of the microstructure (arrangement of particles in water) with increasing shear rate could be more severe because of the possibility of the rearrangement of distorted microstructure during the periodic cycles of the linear dynamic tests.

4.2. Shear thickening behaviour

All samples with polymer volume fractions greater than 44% showed a shear thickening effect. However, performing these same tests on a controlled stress rheometer with a different size (larger gap width) than that of our main rheometer revealed no shear thickening behaviour in the same region of shear rate. This dependence on rheometer geometry has been observed elsewhere [17,19,33–35]. As more recent evidence suggests, this illustrates the idea that stresses in shear thickening suspensions are predominately hydrodynamic, or viscous, in origin, and are due to particle clustering which produces effectively elongated aggregates that dissipate more energy than do non-aggregated spheres. Shear thickening requires not only that sliding layers be broken down by shear, but that the fragments of these layers must rotate and colloid with each other to form structures whose average dimensions in the flow -gradient direction are large. Such structures can 'jam' the flow, leading to abrupt shear thickening. On the other hand, if the particle concentration is not high enough, layer breakdown does not lead to jamming, and there is no abrupt shear thickening.

We found that the shear rate corresponding to the onset of shear thickening onset passes through a local maximum in the solid content equal to ϕ_c for both latices (Fig. 9). This trend is similar to the typical volume fraction dependence of critical shear stress for 'shear thinning' [35], but it apparently is not totally in agreement with the concept of the decreasing of $\dot{\gamma}_c$ for shear thickening with increasing volume fractions [23,33,34,36]. These contradictory results might be due to the fact that not enough data was available in the previous studies to clearly identify ϕ_c.

Jomha et al. [37] reported flow curves showing shear thickening of non-aqueous polystyrene latices. They observed the same type of shear thickening behaviour as observed in the current work in the sense that the onset of shear thickening occurred at a higher shear rate for 55% polymer per unit volume than at 50% and 60%. On the other hand, the experimental results of Catherall et al. [25] show that shear thickening is observed for 55% and 57% volume fraction but the onset of shear thickening for 55% is not presented in their paper.

Thus the observation in Fig. 9 should be reasonable, suggesting that the structure of the latex particles becomes more ordered, stable and more 'stiffer' at this critical concentration where the contacting of double layers began. Consequently, the application of a more intensive shear rate is required to provoke disorder in this structure. Therefore, the usual trend, which considers the decrease of the onset

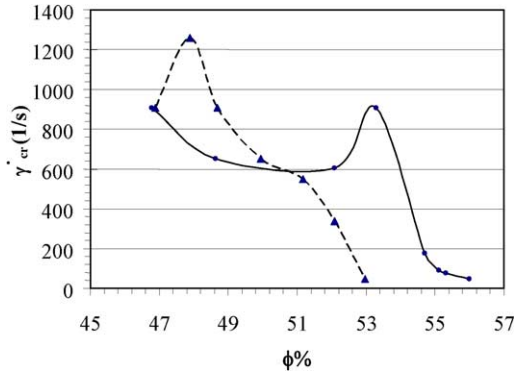

Fig. 9. Shear thickening behaviour: Variation of the critical shear rate versus volume fraction for PS (●) and PSS (▲).

shear thickening with increasing concentration, fails in the region of critical concentration.

5. Conclusion

The rheological behaviour of two series of concentrated latices around of the high critical concentration ϕ_c was investigated. The exact critical volume fractions at which the dispersion changes from viscous to elastic behaviour were clearly identified from the behaviour of the linear complex shear modulus $G^*(\omega)$ at different latex concentrations. However, linear viscoelastic observations suggest that the presence of the electrically charged groups on the surface of PSS induce interactions between neighbouring particles. On the other hand, the PS particles behave more like rigid non-interacting spheres. A percolation threshold can be defined from the variation of the complex shear modulus versus the volume fraction. Effective volume fractions ϕ_{eff} were successfully used to describe the concentration dependence of the relative viscosity data of our two polystyrene latex samples.

Another interesting finding in this work is the good agreement between the experimental value of ϕ_c, related parameters of Krieger–Dougherty equation and the parameters achieved by the percolation theory (scaling law). On the other hand, we found that at concentrations below ϕ_c the latices obey the Cox–Merz rule. Nevertheless $|\eta^*|$ is greater than the steady shear viscosity at $\omega = \dot{\gamma}$ at higher concentrations ($\phi > \phi_c$) and these cases for our two latex (PS, PSS) the shift factor of 25 for shear rate of steady shear viscosity resulted excellent agreement with Cox–Merz rule.

Finally, we observed that the majority of the flow characteristics are consistent with the well-known phenomenon of a shear induced order-to-disordered transition as shear thickening; the dependence of the onset shear rate is in agreement with the investigation of Xu et al. [23] for concentrations above ϕ_c. This behaviour changes around the critical concentration, as observed do other rheological characters. This may arise from this effect that in the critical region of concentration, the spherical particles of latex are more ordered, stable and stiffer; hence the maximum shear rate for destroying this structure is necessary.

References

[1] Krieger IM, Dougherty TJ. Trans soc Rheol 1959;3:137–52.
[2] Flickinger GL, Dairanieh IS, Zukoski CF. J Non-Newtonian Fluid Mech 1999;87:283–305.
[3] Flickinger GL, Zukoski CF. J Rheol 2002;46(2):455–80.
[4] Milkie T, Lok K, Croucher MD. Colloid Polym Sci 1982;260:531–5.
[5] Tadros ThF, Zsednai A. Colloids Surf 1990;49:103–19.
[6] Nashima T, Furusawa K. Colloids Surf 1991;55:149–61.
[7] Raynaud L, Ernst B, Vergé C, Mewis J. J Colloid Interface Sci 1996; 181:11–19.
[8] Chu F, Guillot J, Guyot A. Colloid Polym Sci 1998;276:05–312.
[9] Hone JHE, Howe AM, Whitesides TH. Colloids Surf A: Physicochem Eng Aspects 2000;161:283–306.
[10] Mewis J, Frith WJ, Strivens TA, Russel WB. AIChE J 1989;35: 415–22.
[11] Marshall L, Zukoski CF. J Phys Chem 1990;94:1164–71.
[12] Rueb CJ, Zukoski CF. J Rheol 1998;42:1451–75.
[13] Doolittle A. J Appl Phys 1951;22:1471–5.
[14] Horn FM, Richtering W, Bergenholtz J, Willenbacher N, Wagner NJ. J Colloid Interface Sci 2000;225:166–78.
[15] Horn FM, Richtering W. J Rheol 2000;44(6):1279–92.
[16] Ketz RJ, Prud'homme RK, Graessley WW. Rheol Acta 1988;27: 531–9.
[17] Laun HM, Bung R, Schmidt F. J Rheol 1991;35(6):999–1034.
[18] Boesrma WH, Laven J, Stein HN. J AIChE 1990;36(3):321.
[19] Boersma WH, Baets PJM, Laven J, Stein HN. J Rheol 1991;35(6): 1093–120.
[20] Laun HM. J Non-Newtonian Fluid Mech 1994;54(1–3):87–108.
[21] Chow MK, Zukoski CF. J Rheol 1995;39(1):15–32.
[22] Chow MK, Zukoski CF. J Rheol 1995;39(1):33–60.
[23] Xu J, Jamieson AM, Wang SQ, Qutubuddin S. J Colloid Interface Sci 1996;182:172–8.
[24] Melrose JR, Van Vliet JH, Ball RC. J Dynam Comp Fluids 1998;301–14.
[25] Catherall AA, Melrose JR. J Rheol 2000;44(1):1–25.
[26] Montfort JP, Marin G, Monge Ph. Macromolecules 1986;19:1979–88.
[27] Liang W, Tadros ThF, Luckham PF. J Colloid Interface Sci 1992;1: 131–9.
[28] Tadros ThF, Liang W, Costello B, Luckham PF. Colloids Surf A: Physicochem Eng Aspects 1993;79:105–14.
[29] Stauffer D, Coniglio A, Adam M. Adv Polym Sci 1982;44:103–64.
[30] Winter HH, Mours M. Adv Polym Sci 1997;134:165–234.
[31] Heydel C, Cassagnau P, Michel A. J Rheol 1999;43(3):499–519.
[32] Quemada D. Rheol Acta 1977;16:82–94.
[33] Fritz G, Maranzano BJ, Wagner NJ, Willenbacher N. J Non-Newtonian Fluid Mech 2002;102:149–56.
[34] Fritz G, Schädler V, Willenbacher N, Wagner NJ. Langmuir 2002;18: 6381–90.
[35] Larson RG. The structure and rheology of complex fluids.: Oxford University Press; 1999. Chapter 6.
[36] Mewis J, Biebaut G. J Rheol 2001;45(3):799–813.
[37] Jomha AI, Merrington A, Woodcock LV, Barnes HA, Lips A. Powder Technol 1991;65:343–70.